

# Superconductivity in $\text{LaRh}_2\text{Sn}_2$

**D Britz and A M Strydom**

Highly correlated matter research group, Physics Department, University of Johannesburg,  
PO Box 524, Auckland Park 2006, South Africa

E-mail: amstrydom@uj.ac.za

**Abstract.**  $\text{LaRh}_2\text{Sn}_2$  crystallizes in the centrosymmetric primitive tetragonal crystal structure  $P4/nmm$  (number 129) commonly referred to as the  $\text{CaBe}_2\text{Ge}_2$ -type which was confirmed on our synthesized samples by x-ray diffraction. We report the existence of this superconducting transition in exploratory work and in this study we proceed with a study into the physical properties of this superconducting ground state. Electrical resistance and heat capacity measurements reveal a sharp and well defined superconducting transition at  $T_{sc} = 0.699(7)$  K. The low-temperature heat capacity measurements show  $\text{LaRh}_2\text{Sn}_2$  to be a weakly coupled ( $\lambda_{el-ph} \approx 0.5$ ) bulk BCS superconductor that has an s-wave singlet ground state with an isotropic energy gap such that  $2\Delta/k_B T_{sc} = 3.38(6)$ . From the field dependence of the electrical resistance the upper critical field was estimated to be  $0.127(3)$  T. The calculated penetration depth and coherence length showed that  $\text{LaRh}_2\text{Sn}_2$  is a type-II superconductor, which was confirmed with low temperature magnetization measurements.

## 1. Introduction

The family of compounds  $\text{RT}_2\text{X}_2$  (R = rare-earth element, T = d-block element and X = p-block element) are split into two separate groups according to their crystal structure. One is the body-centred-tetragonal  $\text{ThCr}_2\text{Si}_2$ -type (space group  $I4/mmm$ ) and the other is the primitive tetragonal  $\text{CaBe}_2\text{Ge}_2$ -type (space group  $P4/nmm$ ). Most of the experimental and theoretical work has been done on the compounds that fall into the  $\text{ThCr}_2\text{Si}_2$ -type structures, for this is where the heavy-fermion superconductors are located [1] and references therein. La-based superconductors are not uncommon in the  $\text{ThCr}_2\text{Si}_2$ -type structure formed with Si and Ge, for instance:  $\text{LaPd}_2\text{Ge}_2$ ,  $\text{LaPt}_2\text{Ge}_2$  [2],  $\text{LaNi}_2\text{Ge}_2$  [3],  $\text{LaRh}_2\text{Si}_2$  [4] but of the  $\text{LaT}_2\text{Sn}_2$  compounds which crystallize in the primitive tetragonal structure, where T = Rh is the only one that has been found to be superconducting [5] to date. This work is therefore devoted to studying the physical properties of this particular superconductor.

## 2. Experimental

Polycrystalline samples were prepared with stoichiometric quantities of the starting materials: La (99.99 %), Rh (99.99 %) and Sn (99.9999 %) with the purities quoted in wt. %, on a water cooled Cu hearth in an arc-furnace manufactured by *Edmund Bühler*. In-situ ultra-high purity Ar gas (> 99.999 %) was used during melting procedure. The samples were melted and flipped 4 times in order to promote sample homogeneity. The samples were then wrapped in Ta foil (99.95 %) and sealed in evacuated quartz tubes. Heat treatment was conducted at  $800^\circ\text{C}$  for 5 days and subsequently quenched in water. Powder X-ray diffraction measurements were

performed at room temperature using a Cu radiation source. The resistivity  $\rho(T)$  and specific heat  $C_P(T)$  measurements were performed on a commercial Physical Property Measurement System manufactured by *Quantum Design* (San Diego, USA) equipped with a  $^3\text{He}$  and dilution refrigerator inserts for measurements down to 50 mK. The resistance was measured using the Electronic Transport Option (ETO) preamplifier setup with an ac-current (9.1 Hz with a current amplitude of 0.3 to 0.1 mA depending on the temperature with lower current values used at lower temperatures in order to reduce Joule heating at these temperatures) while the heat capacity was measured using the adiabatic time relaxation method. The magnetization was measured using a commercial Magnetic Property Measurement System equipped with a  $^3\text{He}$  cryostat developed by *iQuantum* (Tsukuba, Japan) manufactured by *Quantum Design* (San Diego, USA).

### 3. Results

Powder x-ray diffraction of the polycrystalline  $\text{LaRh}_2\text{Sn}_2$  was analyzed with a Rietveld refinement and crystallize in the  $\text{CaBe}_2\text{Ge}_2$ -type structure (space group  $P4/nmm$ ) [6] with  $a = 4.5139(1)$  Å and  $c = 10.4824(5)$  Å, shown in figure 1. Within this structure the La atoms occupy the single Ca site (2c), the Rh atoms occupy two distinct Be sites (2c and 2a) and the Sn atoms occupy two distinct Ge-sites (2c and 2b).

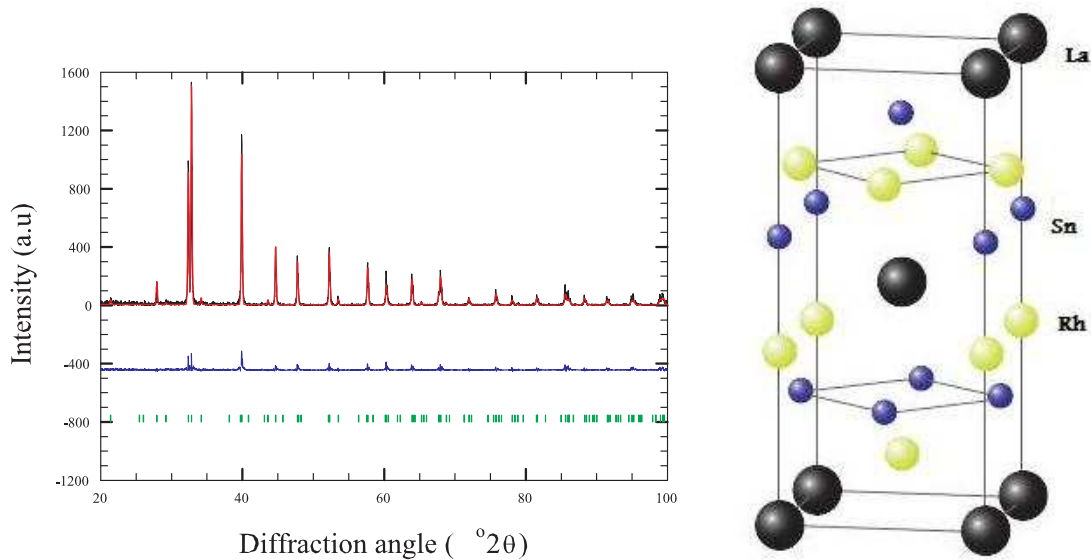


**Figure 1.** Rietveld refinement was performed using the General Structure Analysis System (G.S.A.S) [7] software on x-ray powder diffraction data of  $\text{LaRh}_2\text{Sn}_2$ : the black line representing the experimental spectrum, the red line represents the least-squares fit of the refinement, the blue line is the difference between the experimental data and the fit while the green bars represent the expected peak positions for the  $P4/nmm$  structure. Ball and stick representation of the  $P4/nmm$  structure is shown on the right of the diffractogram.

In the results that follow we follow the convention that the applied field strength  $\mu_0\mathbf{H} =$  magnetic induction  $\mathbf{B}$ . Figure 2 shows the a.c. electrical resistivity that were carried out on a polycrystalline sample of  $\text{LaRh}_2\text{Sn}_2$  in the stated applied magnetic fields, with  $\mathbf{B} \perp \mathbf{j}$  where  $\mathbf{j}$  is the current density. The superconducting transition is clearly visible as the sharp decrease in  $\rho(T)$  around 0.7 K. The transition temperature,  $T_{sc}$ , was taken at the point where the resistance reached half its residual value in the metallic state. Under the application of an external magnetic field, the onset of superconductivity occurred at lower temperatures as expected due to

the pair breaking nature of the magnetic field on the Cooper pairs within the superconducting ground state. The broadening in the width of the transition as the magnetic field is increased is probably due to the appearance of the vortex state within a type-II superconductor.

Inset (a) of figure 2 shows the field dependence of  $T_{sc}$  and this was fitted by [8]:

$$H_c(T) = H_c(0) \left( 1 - \left( \frac{T}{T_{sc}} \right)^2 \right); \quad (1)$$

where  $H_c(0)$  is the critical field at zero temperature. The values obtained from the fit were  $H_c(0) = 0.127(3)$  T and  $T_{sc} = 0.699(7)$  K.

Inset (b) of figure 2 shows the  $\mathbf{B} = 0.11$  T resistivity data where the superconducting transition is no longer visible. The temperature dependence of  $\rho(T)$  becomes proportional to  $T^2$ , which is shown by the dashed red line which serves as a guide to the eye. This temperature dependence in the electrical resistivity is indicative of electron-electron scatterings within a Fermi-liquid state. The application of magnetic field suppresses the superconducting ground state and a Fermi-liquid state emerges.

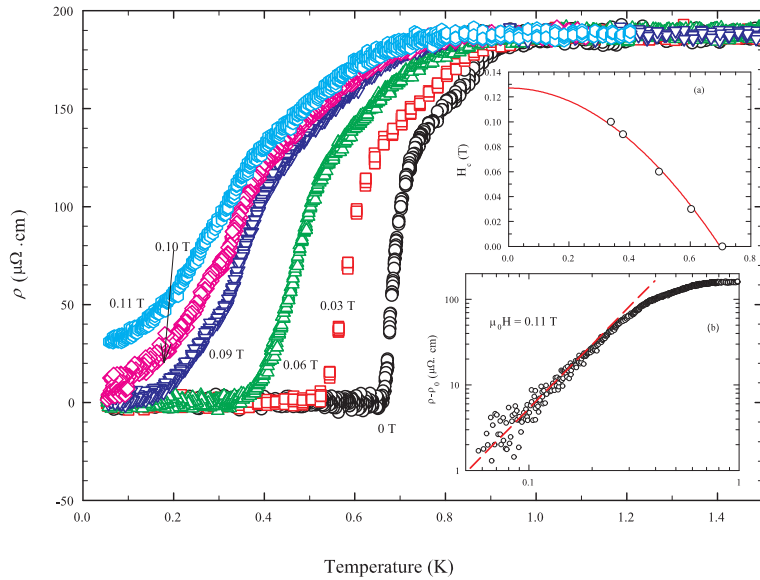


**Figure 2.** Resistivity of  $\text{LaRh}_2\text{Sn}_2$  as a function of temperature in various applied magnetic fields. Inset (a): The critical field plotted as a function of temperature with a fit discussed in the text. Inset (b): Log-log plot of the  $B = 0.11$  T resistivity data with the residual resistivity subtracted, revealing the  $T^2$  dependence shown by the dashed red line which is discussed in the text.

The specific heat measured in applied magnetic fields in the range of 0 to 0.7 T is shown in figure 3. The Debye fit,  $C_p(T)/T = \gamma_N + \beta T^2$ , is shown in inset (a) of figure 3 and returned the following values:  $\gamma_N = 11.796(9)$   $\text{mJ} \cdot \text{mol}^{-1} \text{K}^{-2}$  and  $\beta = 0.816(2)$   $\text{mJ} \cdot \text{mol}^{-1} \text{K}^{-4}$  which corresponds to a Debye temperature  $\theta_D = 228.4(5)$  K. Using the theory outlined by McMillan [9] the electron-phonon coupling is given by:

$$\lambda_{\text{el-ph}} = \frac{1.04 + \mu^* \ln(\theta_D/1.45T_{sc})}{(1 - 0.62\mu^*) \ln(\theta_D/1.45T_{sc}) - 1.04} \quad (2)$$

where  $\mu^*$  represents the screened Coulomb part, which is generally taken to lie within the range of 0.1 to 0.15, and if we use the value for  $\mu^* = 0.13$  [10] then  $\lambda_{\text{el-ph}} \approx 0.5$  which implies that LaRh<sub>2</sub>Sn<sub>2</sub> is a weakly coupled superconductor.

The linear field dependence of the non-superconducting electronic density of states  $\gamma_S$ , which was taken as the value of  $C_p(T)_B/T$  at 0.36 K is shown in inset (b) of figure 3. The linear field dependence is expected for s-wave pairing revealing that LaRh<sub>2</sub>Sn<sub>2</sub> is a fully gapped isotropic superconductor [10].

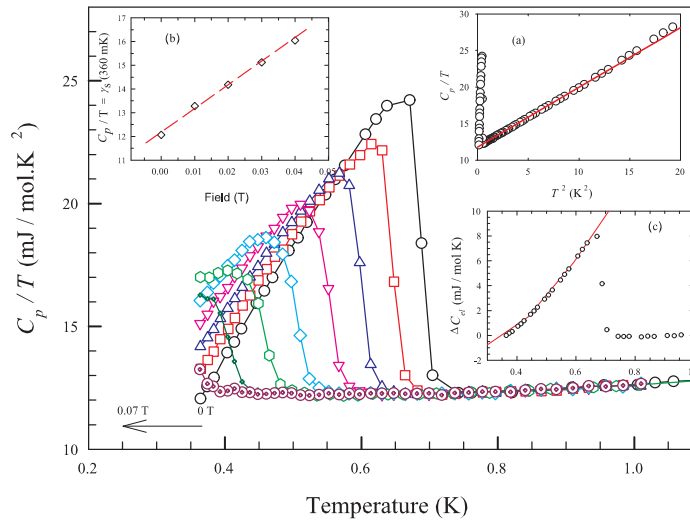


**Figure 3.** Specific heat of LaRh<sub>2</sub>Sn<sub>2</sub> as a function of temperature in various applied magnetic fields (0, 0.01, 0.02, 0.03, 0.04, 0.05, 0.06, 0.07 T) with the solid lines being guides to the eye. Inset (a): Debye fit to the paramagnetic region above the superconducting transition represented by the solid red line. Inset (b): The field dependence of the non-superconducting density of states within the superconducting state with a dashed red line serving as a guide to the eye for the linear-in-**B** dependence. Inset (c): Temperature dependence of the electronic part of the specific heat,  $\Delta C_{\text{el}}(T)$ , for LaRh<sub>2</sub>Sn<sub>2</sub> with the solid red line being a fit that assumed an isotropic s-wave BCS superconducting gap.

Inset (c) of figure 3 shows the electronic part of the specific heat which is obtained from subtracting the Debye spectrum, which was calculated from the specific heat data measured in zero applied field from the measured zero applied field specific heat. The solid red line is a fit of the expected BCS temperature dependence of the electronic specific heat in the superconducting region, namely [8]:

$$\Delta C_{\text{el}}(T) \approx \sqrt{T} e^{-\Delta/k_B T} \quad (3)$$

with  $2\Delta/k_B T_{\text{SC}} = 3.38(6)$  which is in reasonable agreement with the expected weak coupling BCS value of 3.52. The critical field at 0 K is related to the Ginzburg-Landau coherence length ( $\xi_{GL}$ ) by [11]:

$$\xi_{GL}(0) = \left( \frac{\Phi_0}{2\pi H_c(0)} \right)^{1/2}; \quad (4)$$

where  $\Phi_0 = h/2e = 2.07 \times 10^{-15}$  T.m<sup>2</sup> is the flux quantum and by substituting in these respective values one finds  $\xi_{GL}(0) = 50.93$  nm. Together with the parameters obtained from the Debye fit to the specific heat data, inset (a) figure 3, one can find the thermodynamic critical field ( $H_c^*(0)$ ) by using the following relation [11]:

$$H_c^*(0) = 4.23T_{SC}\sqrt{\gamma_N}; \quad (5)$$

with the paramagnetic normal state Sommerfeld coefficient  $\gamma_N = 11.796(9)$  mJ.mol<sup>-1</sup>K<sup>-2</sup> in the case of LaRh<sub>2</sub>Sn<sub>2</sub>. Substituting in these values yields  $H_c^*(0) = 10.155 \times 10^{-3}$  T. The Ginzburg-Landau parameter ( $\kappa_{GL}$ ) at zero temperature is used to identify whether a superconductor is unstable toward vortex formation if  $\kappa_{GL}(0) > 1/\sqrt{2}$  then the vortex state will be stable. The Ginzburg-Landau parameter is given by the following relation [11]:

$$\kappa_{GL}(0) = \frac{H_c(0)}{\sqrt{2}H_c^*} \quad (6)$$

and using the values which were calculated above the value for  $\kappa_{GL}(0) = 8.84$ . This value for  $\kappa_{GL}(0)$  is above  $1/\sqrt{2}$  therefore LaRh<sub>2</sub>Sn<sub>2</sub> is classified as a type-II superconductor. These two relations allows one to find the Ginzburg-Landau penetration depth  $\lambda_{GL}(0) = \xi_{GL}(0)\kappa_{GL}(0)$  which gives  $\lambda_{GL}(0) = 450.22$  nm.

The magnetization below the superconducting transition temperature is shown in figure 4. The low field region has a linear field dependence, which is a result of the perfect diamagnetism that exists in the Meissner state. This linear field dependence terminated around 25 Oe. This field where the Meissner state breaks down is known as the lower critical field  $H_{c1}$  in type-II superconductors and signals the nucleation and growth of the vortices in the vortex state. The slow increase of the magnetization with increasing applied magnetic field is due to the increased density of vortices within the mixed state of a type-II superconductor, as more flux quanta are allowed to penetrate the superconducting state. The hysteresis observed in opposed field runs (positive and negative field polarities), indicated by the arrows, is caused by vortex pinning at the surface of the superconductor. This behaviour confirms that the vortex state exists and that LaRh<sub>2</sub>Sn<sub>2</sub> is a type-II superconductor for there are no vortices present in type-I superconductors.

The value of the gradient of the linear-in-field region (Meissner state) of the  $M(T, B)$  data allows us to estimate the volume fraction that is superconducting. The gradient value corresponding to 100 % superconducting volume fraction is  $-1/4\pi$  (perfect diamagnetism). The calculated gradient revealed that around 84 % of the sample is superconducting at 0.48 K, within error regarding the approximations made with the geometrical factor due to the irregular shape of the sample. This, along with the specific heat measurements, confirmed bulk superconductivity within LaRh<sub>2</sub>Sn<sub>2</sub>.

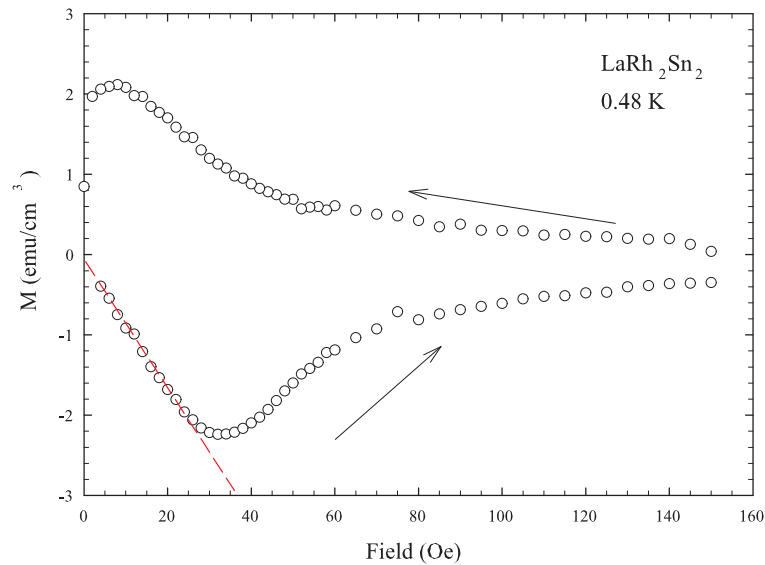


**Figure 4.** Magnetization as a function of applied magnetic field with the arrows indicating the direction of the field sweep. The dashed red line is a straight line to highlight the linear-in- $B$  behaviour at low  $B$ .

#### 4. Conclusion

We have examined the superconducting properties of  $\text{LaRh}_2\text{Sn}_2$  and found it to be a weakly coupled BCS superconductor that is isotropically gapped at the Fermi surface with a transition temperature  $T_{\text{SC}} = 0.699(7)$  K. Above 25 Oe at 0.48 K the vortex state is seen in magnetization measurements which indicated that  $\text{LaRh}_2\text{Sn}_2$  is a type-II superconductor. This behaviour is in line with the Ginzburg-Landau parameter being larger than  $1/\sqrt{2}$  which was calculated from specific heat capacity data. The upper critical field is estimated to be 0.127(3) T from electrical resistance measurements. This BCS behaviour is similar to the other non-4f  $\text{RT}_2\text{X}_2$  ( $\text{R} = \text{La}$ ,  $\text{Y}$  and  $\text{X} = \text{Si}$ ,  $\text{Ge}$ ) superconductors which form in the body-centered tetragonal structure.

#### 5. References

- [1] Stockert *et al* O 2012 *J. Phys. Soc. Jpn.* **81** 011001
- [2] Hull G W, Wernick J H, Geballe T H, Waszczak J V and Bernardini J E 1981 *Phys. Rev. B* **24**(11) 6715–6718  
URL <http://link.aps.org/doi/10.1103/PhysRevB.24.6715>
- [3] Wernick J, Hull G, Geballe T, Bernardini J and Waszczak J 1982 *Materials letters* **1** 71
- [4] Palstra T T M, Lu G, Mcnovsky A A, Nieuwenhuys G J, Kes P H and Mydosh J A 1986 *Phys. Rev. B* **34** 4566
- [5] Strydom A and Britz D 2012 *J. Phys. Soc. Jpn.* **81** SB018
- [6] Francois M, Venturini G, Mareche J, Malaman B and Roques B 1985 *J. Less-Common Met.* **113** 231
- [7] Larson A and Von Dreele R 1994 General structure analysis system (gsas) los alamos national laboratory report laur
- [8] Schrieffer J 1999 *Theory of Superconductivity* Advanced Book Program Series (UK: Advanced Book Program, Perseus Books)
- [9] McMillan W L 1968 *Phys. Rev.* **167**(2) 331–344
- [10] Anand V K, Hillier A D, Adroja D T, Strydom A M, Michor H, McEwen K A and Rainford B D 2011 *Phys. Rev. B* **83**(6) 064522 URL <http://link.aps.org/doi/10.1103/PhysRevB.83.064522>
- [11] Orlando T P, McNiff E J, Foner S and Beasley M R 1979 *Phys. Rev. B* **19**(9) 4545–4561 URL <http://link.aps.org/doi/10.1103/PhysRevB.19.4545>